

Joint Beamforming and Reconfigurable Intelligent Surface Design for Two-Way Relay Networks

Jun Wang, Ying-Chang Liang, *Fellow, IEEE*, Jignon Joung, *Senior Member, IEEE*, Xiaojun Yuan, *Senior Member, IEEE*, and Xinguo Wang

Abstract

In this paper, we consider a reconfigurable intelligent surface (RIS)-assisted two-way relay network, in which two users exchange information through the base station (BS) with the help of an RIS. By jointly designing the phase shifts at the RIS and beamforming matrix at the BS, our objective is to maximize the minimum signal-to-noise ratio (SNR) of the two users, under the transmit power constraint at the BS. We first consider the single-antenna BS case, and propose two algorithms to design the RIS phase shifts and the BS power amplification parameter, namely the SNR-upper-bound-maximization (SUM) method, and genetic-SNR-maximization (GSM) method. When there are multiple antennas at the BS, the optimization problem can be approximately addressed by successively solving two decoupled subproblems, one to optimize the RIS phase shifts, the other to optimize the BS beamforming matrix. The first subproblem can be solved by using SUM or GSM method, while the second subproblem can be solved by using optimized beamforming or maximum-ratio-beamforming method. The proposed algorithms have been verified through numerical results with computational complexity analysis.

Part of this work was presented in IEEE Globecom 2020 [1]. This work has been submitted to the IEEE for possible publication. Copyright may be transferred without notice, after which this version may no longer be accessible.

J. Wang is with the National Key Laboratory of Science and Technology on Communications, and the Center for Intelligent Networking and Communications (CINC), University of Electronic Science and Technology of China (UESTC), Chengdu 611731, China (e-mail: junwang@std.uestc.edu.cn). Y.-C. Liang and X.-J. Yuan are with the Center for Intelligent Networking and Communications (CINC), University of Electronic Science and Technology of China (UESTC), Chengdu 611731, China (e-mail: liangyc@ieee.org and xjyuan@uestc.edu.cn). J. Joung is with the School of Electrical and Electronics Engineering, Chung-Ang University, Seoul 06974, South Korea (e-mail: jgjoung@au.ac.kr). X.-G. Wang is with the School of Computer Science, Chengdu University of Information Technology, Chengdu 610025, China, and also with the Center for Intelligent Networking and Communications (CINC), and National Key Laboratory of Science and Technology on Communications, University of Electronic Science and Technology of China, Chengdu, China (e-mail: xinguowang911@163.com).

Index Terms

Two-way relay network, reconfigurable intelligent surface, genetic algorithm.

I. INTRODUCTION

The *sixth generation* (6G) mobile networks are expected to support peak data rate of terabits per second and millions of wireless connections per square kilometer [2]–[4]. The exponential growth of the wireless traffic and communication device thus call for novel spectral- and energy-efficient technologies for future wireless communications [5]. Recently, *reconfigurable intelligent surface* (RIS), also known as an intelligent reflecting surface, has become a promising technique to help to fulfill these requirements [6]–[8]. The rise of the RIS technique is closely related to the fast development of the meta-materials and the fabrication technology. Through intelligently adjusting the phase shifts of RIS, the wireless channels become programable and controllable. Thus RIS can be applied to various wireless communication systems to assist the performance improvement, and the study of RIS techniques has been attracting more and more attention from the industry and academia.

In [9], RIS was used to achieve up to three times higher energy efficiency compared with conventional *amplify-and-forward* (AF) relay. RIS was applied to wireless systems to achieve enhanced physical layer security in [10], [11]. The confidential data streams were transmitted to the legitimate receivers while keeping them secret from the eavesdroppers with the help of the RIS. RIS-aided multi-user downlink *multiple-input single-output* (MISO) system was investigated in [12]. The weighted sum rate was maximized by jointly designing the transmit beamforming and RIS phase shifts under the perfect and imperfect *channel state information* (CSI) setup. The max-min fairness problem was considered in the RIS-aided multi-cell MISO systems [13]. In [14], the RIS-assisted multiuser full-duplex cognitive radio network was investigated. The secondary network employs a full-duplex BS to serve multiple half-duplex downlink and uplink secondary users simultaneously. Here, an RIS is deployed to improve the performance of the secondary network and mitigate the interference to the primary network. In [15], the power control problem was investigated for a physical-layer broadcasting scenario. The RIS-aided multi-group multicast MISO communication system was considered to maximize the sum rate of all the multicasting groups in [16]. Also, the RIS-assisted symbiotic radio for an IoT communication

system was proposed in [17]. RIS-assisted non-orthogonal multiple access system was studied in [18], [19]. In [20], the joint active and passive precoding design for the RIS-assisted *millimeter wave* (mmWave) communication was addressed by exploiting some important characteristics of mmWave channels for both single RIS and multi-RIS cases. The channel capacity optimization in indoor mmWave environments using RIS was studied in [21].

On the other hand, *two-way relay network* (TWRN) is another promising strategy to improve the spectral efficiency in cooperative networks [22], [23]. In TWRN, two phases are required to exchange information between two users through a *two-way relay* (TWR). Here, the key challenge is how to design the beamforming matrix at the TWR. In [24] and its conference version [23], the authors derived the optimal structure of the beamforming matrix at the TWR and provided several sub-optimal schemes to maximize the sum-rate. The beamforming design for the *multiple-input multiple-output* (MIMO) TWR communications to maximize the minimum end-to-end *signal-to-noise ratio* (SNR) was investigated in [25]. The problem was recast as a fractional programming problem and solved by using the Dinkelbach-type procedure combined with semi-definite programming. The beamforming design for multi-user TWR was studied in [26] through a max-min *signal-to-interference-plus-noise ratio* (SINR) problem. The relay processing and power control problem for a multi-user two-way MIMO communication system was investigated in [27].

The existing studies on RIS-assisted TWRN mainly exploited the RIS to replace the conventional relay to realize the information exchange between two users. Specifically, an RIS-assisted full-duplex MIMO TWRN system was investigated in [28], in which both users receive and transmit signals at the same time with the help of the RIS. In [29], the authors analyzed the performance for reciprocal and non-reciprocal channels in the RIS-assisted TWRN system and derived the closed-form expressions for the outage probability and the spectral efficiency when the RIS is equipped with one reflective element. A more general case was studied in [30], in which multiple full-duplex users exchange information with the full-duplex *base station* (BS) with the assist of the RIS. As reported in reference [31], however, the benefit of RIS is conditioned on the proper self-interference cancellation at the full-duplex TWR node, which brings high hardware complexity and low energy efficiency. In [31], an RIS-enhanced two-way orthogonal-frequency-division multiplexing communication system with multiple pairs of users was investigated. By separating the available bandwidth into multiple orthogonal subbands and allocating them to the

user pairs, the two-way device-to-device communication was accomplished.

In this paper, we investigate RIS-assisted TWRN, in which a multi-antenna BS serves two users to exchange information with the help of an RIS, where the BS and RIS can be considered as an active and passive TWRs, respectively. When any of the two links from the users to the BS is weak due to deep fading and shadowing, the RIS can enhance the weak link and provide fairness to both users. By intelligently reconfiguring the reflective elements on the RIS, the information exchange rate can be significantly improved. Here, our objective is to jointly design the beamforming and phase shift matrices at the BS and RIS, respectively, such that the minimum SNR of the two users is maximized under the transmit power constraint at the BS. When solving the optimization problem, the beamforming and phase shift matrices are coupled with each other, and the optimization problem is non-convex. To obtain a design insight, we first study the RIS phase shifts and power amplification parameter design for single-antenna BS case. We first propose the *SNR-upper-bound-maximization* (SUM) algorithm which maximizes an upper bound of the original objective function, namely, the minimum of the combined channel gains seen by the two users. After that, an improved algorithm, called *genetic-SNR-maximization* (GSM) algorithm, is proposed to solve the original problem approximately. When there are multiple antennas at the BS, the optimization problem can be approximately addressed by successively solving two decoupled subproblems, one to optimize the phase shift matrix at the RIS, one to optimize the beamforming matrix at the BS. The RIS phase shifts can be obtained by employing SUM or GSM method while the BS beamforming matrix can be obtained by *optimized beamforming* (OB) or *maximum-ratio-beamforming* (MRB) method. The main contributions of this study are summarized as follows.

- The RIS is applied as a passive TWR into TWRN to improve the information exchange rate.
- The joint beamforming and RIS design problem for RIS-assisted TWRN is formulated to maximize the minimum SNR of the two users under the BS transmit power constraint.
- To obtain the proper insight on the formulated optimization problem, the single-antenna BS case is first investigated. Since the problem is non-convex, we propose to maximize an upper bound of the original objective function, i.e., the minimum of the combined channel gains of the two users. The SUM and GSM algorithms are proposed to solve the design problem.

- For the multiple-antenna BS case, the optimization problem is divided into two decoupled subproblems, one to optimize the RIS phase shifts, the other to optimize the BS beamforming matrix. The SUM and GSM methods are employed to obtain the RIS phase shifts while the OB and MRB methods are employed to obtain the BS beamforming matrix.
- Numerical results verify that the proposed algorithms with RIS can improve the information exchange rate significantly in TWRN.

TABLE I

LIST OF ABBREVIATIONS

Abbreviation	Description
AF	Amplify-and-Forward
AoA	Angle of Arrival
AoD	Angle of Departure
BS	Base Station
CDF	Cumulative Distribution Function
GSM	Genetic-SNR-Maximization
GSM-MRB	Genetic-SNR-Maximization Maximum-Ratio-Beamforming
GSM-OB	Genetic-SNR-Maximization Optimized-Beamforming
MIMO	Multiple-input Multiple-output
MISO	Multiple-input Single-output
mmWave	millimeter Wave
MRR-MRT	Maximal-Ratio-Reception Maximal-Ratio-Transmission
RIS	Reconfigurable Intelligent Surface
SINR	Signal to Interference plus Noise Ratio
SNR	Signal to Noise Ratio
SUM	SNR-Upper-bound-Maximization
SUM-MRB	SNR-Upper-bound-Maximization Maximum-Ratio-Beamforming
SUM-OB	SNR-Upper-bound-Maximization Optimized-Beamforming
TWR	Two-Way Relay
TWRN	Two-Way Relay Network
6G	Sixth Generation

The rest of this paper is organized as follows. Section II presents the system model for the RIS-assisted two-way relay network and provides a joint design optimization problem. In

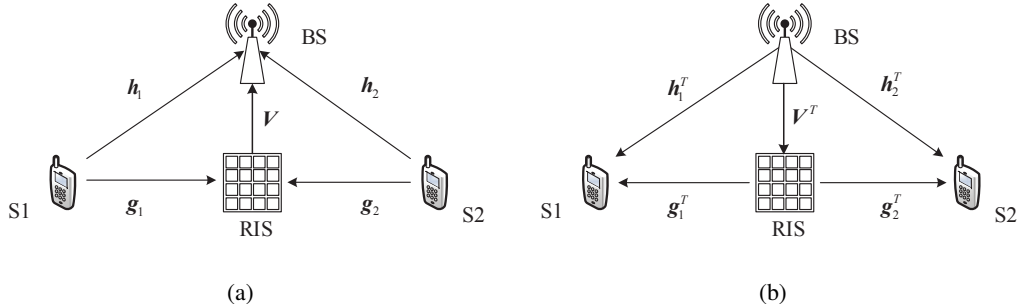


Fig. 1. The system model for the RIS-assisted two-way relay network. (a) First phase: two users send information to the BS with the help of an RIS; (b) Second phase: The BS broadcasts the processed signal to the users with the help of an RIS.

Section III, the single-antenna BS case is presented to obtain insights into the original problem. In Section IV, the algorithms to solve a problem for the multiple-antenna BS case are proposed. Section V provides simulation results to validate the effectiveness of the proposed algorithms. Section VI concludes this study.

Notations: For complex vector \mathbf{v} , \mathbf{v}^* , \mathbf{v}^T , \mathbf{v}^H , and $\text{diag}(\mathbf{v})$ denote the conjugate, the transpose, the conjugate transpose, and the diagonal matrix with its diagonal elements given by \mathbf{v} . Scalar v_i denotes the i th element of vector \mathbf{v} . $[\mathbf{v}]_{(1:N)}$ denotes the first N elements of vector \mathbf{v} . $\mathbf{a} \otimes \mathbf{b}$ denotes the Kronecker product of vector \mathbf{a} and \mathbf{b} . $\text{vec}(\mathbf{A})$ denotes the vectorization operation for matrix \mathbf{A} . \mathbf{A}^* denotes the optimal value of variable \mathbf{A} . $\text{tr}(\mathbf{A})$ and $\text{rank}(\mathbf{A})$ denote the trace and rank of the matrix \mathbf{A} , respectively. $\mathbf{A}[m, n]$ and $\mathbf{A}[m, :]$ denote the (m, n) th element and the m th row vector of matrix \mathbf{A} , respectively. $\mathbf{A} \succeq 0$ denotes that matrix \mathbf{A} is a semi-definite matrix. The distribution of a *circularly symmetric complex Gaussian* (CSCG) random variable with mean μ and variance σ^2 is denoted by $\mathcal{CN}(\mu, \sigma^2)$. Finally, the list of abbreviations appeared in this paper is given in Table I.

II. SYSTEM MODEL

In this paper, we consider an RIS-assisted TWRN. As illustrated in Fig. 1, the system consists of a BS with M antennas, two single-antenna users, i.e., the source nodes denoted by S1 and S2, and an RIS with N reflective elements, each of which can introduce a phase shift to the incident signal. Two users exchange information with the help of the BS and RIS, where the BS and RIS operate as active and passive TWRs, respectively. The RIS is deployed to enhance the TWR channels between the users and the BS so that the information exchange rate can be

improved. In the following, we present the channel and the signal models of the RIS-assisted TWRN considered in this study.

A. Channel Model

We assume the flat fading channels, which means that the channels remain unchanged during one transmission block. The channels from S1 and S2 to the BS are respectively denoted by $\mathbf{h}_1 \in \mathbb{C}^{M \times 1}$ and $\mathbf{h}_2 \in \mathbb{C}^{M \times 1}$, which are modeled as the Rayleigh channels. Here, it is assumed that the *line-of-sight* (LoS) path is blocked. The elements of the channels are independent and follow a distribution of $\sqrt{\eta(d_{B,k})}\mathcal{CN}(0, 1)$, $k = 1, 2$, where $\eta(d_{B,k})$ denotes the large-scale path loss component of the channels depending on the distance $d_{B,k}$ between user k and the BS. The channels from S1 to RIS, from S2 to RIS, and from RIS to BS are denoted by $\mathbf{g}_1 \in \mathbb{C}^{N \times 1}$, $\mathbf{g}_2 \in \mathbb{C}^{N \times 1}$, and $\mathbf{V} \in \mathbb{C}^{M \times N}$, respectively. Since the LoS path exists in these channels, the channels are modeled as the Rician channels, without loss of generality, i.e.,

$$\mathbf{V} = \sqrt{\eta(d_{B,R})} \left(\sqrt{\frac{K_v}{1+K_v}} \mathbf{V}^{\text{LoS}} + \sqrt{\frac{1}{1+K_v}} \mathbf{V}^{\text{NLoS}} \right), \quad (1)$$

and

$$\mathbf{g}_k = \sqrt{\eta(d_{k,R})} \left(\sqrt{\frac{K_k}{1+K_k}} \mathbf{g}_k^{\text{LoS}} + \sqrt{\frac{1}{1+K_k}} \mathbf{g}_k^{\text{NLoS}} \right), \quad k = 1, 2, \quad (2)$$

where $d_{B,R}$ is the distance between RIS and BS, and $d_{k,R}$ is the distance between user k and RIS. The small-scale component consists of the LoS and non-LoS (NLoS) components. K_v and K_k are the Rician factors of \mathbf{V} and \mathbf{g}_k , respectively. $\mathbf{V}^{\text{LoS(NLoS)}}$ and $\mathbf{g}_k^{\text{LoS(NLoS)}}$ denote the LoS (NLoS) components of \mathbf{V} and \mathbf{g}_k , respectively. The NLoS components follow the standard complex Gaussian distribution with zero mean and unit variance. The LoS components can be expressed by the responses of the RIS.

Since the RIS is a uniform rectangular array, the steering vector $\mathbf{a}_R(\theta, \psi)$ at the RIS is modeled as follows:

$$\mathbf{a}_R(\theta, \psi) = \mathbf{a}_v(\theta, \psi) \otimes \mathbf{a}_h(\theta, \psi) \in \mathbb{C}^{1 \times N}, \quad (3)$$

where θ and ψ denote the center azimuth and elevation angles, respectively, of the arriving or departing signals at the RIS; $\mathbf{a}_h(\theta, \psi) \in \mathbb{C}^{1 \times N_h}$ and $\mathbf{a}_v(\theta, \psi) \in \mathbb{C}^{1 \times N_v}$ are the steering vectors in the horizontal and vertical directions, respectively [32]; N_h and N_v are the numbers of elements

along the horizontal and vertical axes, respectively. Here, the elements of \mathbf{a}_h and \mathbf{a}_v can be modeled, respectively, as

$$[\mathbf{a}_h(\theta, \psi)]_n = e^{-j\frac{2\pi d}{\lambda}(n-1)\cos(\psi)\sin(\theta)}, \forall n \in \{1, 2, \dots, N_h\}, \quad (4)$$

$$[\mathbf{a}_v(\theta, \psi)]_n = e^{j\frac{2\pi d}{\lambda}(n-1)\cos(\psi)\cos(\theta)}, \forall n \in \{1, 2, \dots, N_v\}, \quad (5)$$

where d and λ are the antenna element separation and carrier wavelength, respectively. On the other hand, since BS employs a horizontal linear array, i.e., $\psi = 0$, the steering vector at the BS is modeled as

$$\mathbf{a}_B(\theta_{\text{AoA,B}}) = [1, e^{-j\frac{2\pi d}{\lambda}\sin(\theta_{\text{AoA,B}})}, \dots, e^{-j\frac{2\pi d}{\lambda}(M-1)\sin(\theta_{\text{AoA,B}})}] \in \mathbb{C}^{1 \times M}, \quad (6)$$

where $\theta_{\text{AoA,B}}$ denotes the *angle of arrival* (AoA) at the BS. d is set as $d = \frac{1}{2}\lambda$ for simplicity.

Using the steering vectors in (3) and (6), the LoS channels are modeled as follows:

$$\mathbf{V}^{\text{LoS}} = \mathbf{a}_B^H(\theta_{\text{AoA,B}}) \mathbf{a}_R(\theta_{\text{AoD,R}}, \psi_{\text{AoD,R}}), \quad (7)$$

where $\theta_{\text{AoD,R}}$ and $\psi_{\text{AoD,R}}$ denote the center azimuth *angle of departure* (AoD) and elevation AoD, respectively, at the RIS and

$$\mathbf{g}_k^{\text{LoS}} = \mathbf{a}_R^H(\theta_{\text{AoA},k}, \psi_{\text{AoA},k}), k = 1, 2, \quad (8)$$

where $\theta_{\text{AoA},k}$ and $\psi_{\text{AoA},k}$ denote the center azimuth and elevation AoAs, respectively, at the RIS for user k .

B. Signal Model

Under a time-division-duplex mode, two phases are needed for the two users to exchange information. In the first phase, two users send their information to the BS, simultaneously, with the help of an RIS as shown in Fig. 2(a). In the second phase, the BS performs beamforming for the signal received in the first phase and broadcasts the processed signal to the users, as shown in Fig. 2(b). Two users then decode the received signals, and the information exchange is completed.

In the first phase, the BS received signal is given by

$$\mathbf{r} = \sqrt{P_S}(\mathbf{h}_1 + \mathbf{V}\Phi_1\mathbf{g}_1)x_1 + \sqrt{P_S}(\mathbf{h}_2 + \mathbf{V}\Phi_1\mathbf{g}_2)x_2 + \mathbf{u}, \quad (9)$$

where Φ_1 denotes a diagonal phase shift matrix at RIS at the first phase; P_S is the transmit power of users; and $\mathbf{u} \in \mathbb{C}^{M \times 1} \sim \mathcal{CN}(0, \sigma^2 \mathbf{I})$ is the additive complex noise vector; and x_1 and x_2 denote the information signal of S1 and S2, respectively. Here, it is assumed that x_1 and x_2 conform to the same distribution $\mathcal{CN}(0, 1)$. After receiving the signal \mathbf{r} , the BS performs beamforming to generate the retransmit signal as follows:

$$\mathbf{s} = \mathbf{A}\mathbf{r}, \quad (10)$$

where $\mathbf{A} \in \mathbb{C}^{M \times M}$ denotes the beamforming matrix¹.

In the second phase, assuming that the channel reciprocity holds during the first and second phases, the second-phase channel can be modeled as the transpose of the first-phase channel. Denoting the phase shift matrix at the second phase by Φ_2 , the received signal at S1 is then written as follows:

$$\begin{aligned} y_1 &= (\mathbf{h}_1 + \mathbf{V}\Phi_2\mathbf{g}_1)^T \mathbf{s} + z_1 \\ &= \sqrt{P_S}(\mathbf{h}_1 + \mathbf{V}\Phi_2\mathbf{g}_1)^T \mathbf{A}(\mathbf{h}_1 + \mathbf{V}\Phi_1\mathbf{g}_1)x_1 + \sqrt{P_S}(\mathbf{h}_1 + \mathbf{V}\Phi_2\mathbf{g}_1)^T \mathbf{A}(\mathbf{h}_2 + \mathbf{V}\Phi_1\mathbf{g}_2)x_2 \\ &\quad + (\mathbf{h}_1 + \mathbf{V}\Phi_2\mathbf{g}_1)^T \mathbf{A}\mathbf{u} + z_1. \end{aligned} \quad (11)$$

Since S1 knows its own signal and CSI $(\mathbf{h}_1 + \mathbf{V}\Phi_2\mathbf{g}_1)^T \mathbf{A}(\mathbf{h}_1 + \mathbf{V}\Phi_1\mathbf{g}_1)$ following the signaling and channel estimation in [34], x_1 can be canceled from the received signal, i.e., self-interference cancellation, yielding

$$\tilde{y}_1 = \sqrt{P_S}(\mathbf{h}_1 + \mathbf{V}\Phi_2\mathbf{g}_1)^T \mathbf{A}(\mathbf{h}_2 + \mathbf{V}\Phi_1\mathbf{g}_2)x_2 + (\mathbf{h}_1 + \mathbf{V}\Phi_2\mathbf{g}_1)^T \mathbf{A}\mathbf{u} + z_1. \quad (12)$$

Similarly, the signal received by S2 after self-interference cancellation is given by

$$\tilde{y}_2 = \sqrt{P_S}(\mathbf{h}_2 + \mathbf{V}\Phi_2\mathbf{g}_2)^T \mathbf{A}(\mathbf{h}_1 + \mathbf{V}\Phi_1\mathbf{g}_1)x_1 + (\mathbf{h}_2 + \mathbf{V}\Phi_2\mathbf{g}_2)^T \mathbf{A}\mathbf{u} + z_2. \quad (13)$$

Here, \mathbf{u} , z_1 , and z_2 are independent, where z_1 and z_2 conform to the distribution $\mathcal{CN}(0, \sigma^2)$.

The SNR at S1 can then be derived as follows:

$$\gamma_1 = \frac{P_S |(\mathbf{h}_1 + \mathbf{V}\Phi_2\mathbf{g}_1)^T \mathbf{A}(\mathbf{h}_2 + \mathbf{V}\Phi_1\mathbf{g}_2)|^2}{\|(\mathbf{h}_1 + \mathbf{V}\Phi_2\mathbf{g}_1)^T \mathbf{A}\|^2 \sigma^2 + \sigma^2} = \frac{\beta |(\mathbf{h}_1 + \mathbf{V}\Phi_2\mathbf{g}_1)^T \mathbf{A}(\mathbf{h}_2 + \mathbf{V}\Phi_1\mathbf{g}_2)|^2}{\|(\mathbf{h}_1 + \mathbf{V}\Phi_2\mathbf{g}_1)^T \mathbf{A}\|^2 + 1}, \quad (14)$$

¹The BS acts as an AF relay in the TWRN since the AF relay requires much less delay and computing power compared to a decode-and-forward relay [33].

where $\beta = P_S/\sigma^2$. Similarly, the SNR at S2 is

$$\gamma_2 = \frac{\beta |(\mathbf{h}_2 + \mathbf{V}\Phi_2\mathbf{g}_2)^T \mathbf{A}(\mathbf{h}_1 + \mathbf{V}\Phi_1\mathbf{g}_1)|^2}{\|(\mathbf{h}_2 + \mathbf{V}\Phi_2\mathbf{g}_2)^T \mathbf{A}\|^2 + 1}. \quad (15)$$

We have the following proposition.

Proposition 1: During consecutive two-phase transmissions, we design the phase shifts, such that they do not vary over the two phases, i.e. $\Phi_1 = \Phi_2 = \Phi = \text{diag}(e^{j\theta_1}, e^{j\theta_2}, \dots, e^{j\theta_N})$ where θ_i denotes the phase shift introduced by the i th RIS element.

Proof: See proof in Appendix A. ■

The transmit power at BS is given by

$$P(\mathbf{A}, \Phi) = \text{tr}[\mathbf{s}\mathbf{s}^H] = P_S \|\mathbf{A}(\mathbf{h}_1 + \mathbf{V}\Phi\mathbf{g}_1)\|^2 + P_S \|\mathbf{A}(\mathbf{h}_2 + \mathbf{V}\Phi\mathbf{g}_2)\|^2 + \sigma^2 \text{tr}(\mathbf{A}\mathbf{A}^H). \quad (16)$$

Remark 1: For the more general case in which a large number of users must be served, two users are paired each time to realize an exchange of information. By allocating orthogonal resources, such as time and frequency, to different two-user pairs, i.e., TDMA and OFDMA, the proposed algorithms for a single pair of two users in the two-way communications can be directly extended to the multiple two-user pairs. Without the assistance of the RIS, the scenario is conventional multipair two-way relay network and there are already several researches working on this, such as [35].

C. Discussion on Channel State Information Acquisition

To optimize the beamforming matrix \mathbf{A} and the phase shift matrix Φ , the RIS-assisted TWRN system needs to acquire the CSI. In the literature, the CSI of the RIS channels can be obtained through, e.g., the Brute-Force method [36], the compressive-sensing method [37], and the semi-passive RIS method [38]. From the channel reciprocity during the uplink and downlink, the second-phase channel can be obtained by taking the transpose of the first-phase channel. Here, the channel estimation error can be tackled by using a robust design method, e.g., [39].

D. Problem Formulation

To maximize the information exchange rate while considering fairness between two users, the minimum SNR of the two users is maximized by jointly optimizing beamforming matrix \mathbf{A}

TABLE II
PROPOSED ALGORITHMS THROUGHOUT THE PAPER

Algorithms Scenarios	Optimizing Φ	Optimizing \mathbf{A}	Section
Single-antenna BS case	SUM	Formula (21)	Section III-A: SUM
	GSM		Section III-B: GSM
Multiple-antenna BS case	SUM	OB	Section IV-A: SUM-OB
		MRB	Section IV-B: SUM-MRB
	GSM	OB	Section IV-C: GSM-OB
		MRB	Section IV-C: GSM-MRB

and phase shift matrix Φ at BS and RIS, respectively, subject to the transmit power constraint at the BS. Denoting the transmit power budget at the BS by P_B , the optimization problem is formulated as follows:

$$\begin{aligned}
 (\mathbf{Po}) : \max_{\Phi, \mathbf{A}} \quad & \min \{ \gamma_1, \gamma_2 \} \\
 \text{s.t.} \quad & |\phi_n| = 1, \forall n,
 \end{aligned} \tag{17a}$$

$$\beta \|\mathbf{A}(\mathbf{h}_1 + \mathbf{V}\Phi\mathbf{g}_1)\|^2 + \beta \|\mathbf{A}(\mathbf{h}_2 + \mathbf{V}\Phi\mathbf{g}_2)\|^2 + \text{tr}(\mathbf{A}\mathbf{A}^H) \leq \frac{P_B}{\sigma^2}. \tag{17b}$$

This problem is challenging to be directly solved because BS beamforming matrix \mathbf{A} and phase shift matrix Φ are coupled to each other. The quadratic term of Φ in the numerator of the SNR in (14) and (15) makes the problem even more intractable. To solve the optimization problem (\mathbf{Po}) , henceforth, we propose several efficient algorithms, which are as shown in Table II.

III. RIS FOR SINGLE-ANTENNA BS

To obtain some insights on how to solve the problem (\mathbf{Po}) in (17) and design the system, we first study the single-antenna BS case. In this case, the channel matrix $\mathbf{V} \in \mathbb{C}^{M \times N}$ from RIS to BS degenerates to a vector, denoted by $\mathbf{v} \in \mathbb{C}^{1 \times N}$. Moreover, beamforming matrix \mathbf{A} reduces to a power amplification parameter τ , which means that the BS amplifies the received signal without beamforming. The original problem is thus simplified to a problem of how to obtain the RIS phase shift matrix, Φ , and BS power amplification parameter τ . For the single-antenna BS

case, the BS power constraint in (17b) is written as

$$\tau(P_S|h_1 + \mathbf{v}\Phi\mathbf{g}_1|^2 + P_S|h_2 + \mathbf{v}\Phi\mathbf{g}_2|^2 + \sigma^2) \leq P_B. \quad (18)$$

The SNRs at S1 and S2 in (14) and (15) are then derived respectively as follows:

$$\gamma_{S1} = \frac{\beta\tau|(h_1 + \mathbf{v}\Phi\mathbf{g}_1)^T(h_2 + \mathbf{v}\Phi\mathbf{g}_2)|^2}{\tau|h_1 + \mathbf{v}\Phi\mathbf{g}_1|^2 + 1}, \quad (19)$$

$$\gamma_{S2} = \frac{\beta\tau|(h_2 + \mathbf{v}\Phi\mathbf{g}_2)^T(h_1 + \mathbf{v}\Phi\mathbf{g}_1)|^2}{\tau|h_2 + \mathbf{v}\Phi\mathbf{g}_2|^2 + 1}. \quad (20)$$

Since the SNRs of both users increase as τ increases, for a given phase shift matrix Φ , the optimal power amplification parameter is obtained from the equality in (18) as

$$\tau = \frac{P_B}{P_S|h_1 + \mathbf{v}\Phi\mathbf{g}_1|^2 + P_S|h_2 + \mathbf{v}\Phi\mathbf{g}_2|^2 + \sigma^2}. \quad (21)$$

Using (18)–(20), problem (\mathbf{P}_0) for the single-antenna BS case is then rewritten as follows:

$$\begin{aligned} (\mathbf{P}_s - 1) : \max_{\Phi} \quad & \min \{\gamma_{S1}, \gamma_{S2}\} \\ \text{s.t.} \quad & |\phi_n| = 1, \forall n. \end{aligned} \quad (22)$$

Problem $(\mathbf{P}_s - 1)$ is still intractable because the quadratic term of the phase shift matrix still exists in the SNR. Thus, we consider the upper bounds of the SNRs as follows:

$$\begin{aligned} \gamma_{S1} &= \frac{\beta\tau|h_1 + \mathbf{v}\Phi\mathbf{g}_1|^2|h_2 + \mathbf{v}\Phi\mathbf{g}_2|^2}{\tau|h_1 + \mathbf{v}\Phi\mathbf{g}_1|^2 + 1} = \frac{\beta|h_1 + \mathbf{v}\Phi\mathbf{g}_1|^2|h_2 + \mathbf{v}\Phi\mathbf{g}_2|^2}{|h_1 + \mathbf{v}\Phi\mathbf{g}_1|^2 + \frac{1}{\tau}} \\ &= \frac{\beta|h_1 + \mathbf{v}\Phi\mathbf{g}_1|^2|h_2 + \mathbf{v}\Phi\mathbf{g}_2|^2}{|h_1 + \mathbf{v}\Phi\mathbf{g}_1|^2 + \frac{P_S|h_1 + \mathbf{v}\Phi\mathbf{g}_1|^2 + P_S|h_2 + \mathbf{v}\Phi\mathbf{g}_2|^2 + \sigma^2}{P_B}} = \frac{\beta|h_2 + \mathbf{v}\Phi\mathbf{g}_2|^2}{1 + \frac{P_S}{P_B} + \frac{P_S}{P_B} \frac{|h_2 + \mathbf{v}\Phi\mathbf{g}_2|^2}{|h_1 + \mathbf{v}\Phi\mathbf{g}_1|^2} + \frac{\sigma^2}{P_B|h_1 + \mathbf{v}\Phi\mathbf{g}_1|^2}} \\ &\leq \beta|h_2 + \mathbf{v}\Phi\mathbf{g}_2|^2 \triangleq \bar{\gamma}_{S1}. \end{aligned} \quad (23)$$

Similarly, the upper bound of γ_{S2} is derived as $\bar{\gamma}_{S2} \triangleq \beta|h_1 + \mathbf{v}\Phi\mathbf{g}_1|^2$. Because the upper bounds of SNRs are tight when the transmit power of the BS is much greater than that of users, i.e., $P_B \gg P_S$, and this is a typical case of TWRN, the upper bound of SNRs can be used to design the TWRN. Meanwhile, the optimality loss does not highly depend on the tightness of the upper bound. Thus, we devise two algorithms to solve $(\mathbf{P}_s - 1)$ by maximizing the upper bound of SNRs.

A. SNR-Upper-bound-Maximization (SUM) Algorithm

The proposed SUM algorithm solves the following problem:

$$\begin{aligned}
 (\mathbf{Ps} - 2) : \max_{\Phi} \quad & \min \{ \bar{\gamma}_{S1}, \bar{\gamma}_{S2} \} \\
 \text{s.t.} \quad & |\phi_n| = 1, \forall n.
 \end{aligned} \tag{24}$$

Denoting a phase shift vector as $\phi = [e^{j\theta_1}, e^{j\theta_2}, \dots, e^{j\theta_N}]^T \in \mathbb{C}^{N \times 1}$, the combined channel $h_1 + \mathbf{v}\Phi\mathbf{g}_1$ can be written as

$$h_1 + \mathbf{v}\Phi\mathbf{g}_1 = h_1 + \mathbf{v}\text{diag}(\mathbf{g}_1)\phi = [\mathbf{v}\text{diag}(\mathbf{g}_1), h_1][\phi^T, 1]^T \triangleq \bar{\mathbf{g}}_1^H \bar{\phi}, \tag{25}$$

where $[\mathbf{v}\text{diag}(\mathbf{g}_1), h_1] \triangleq \bar{\mathbf{g}}_1^H \in \mathbb{C}^{1 \times (N+1)}$ and $[\phi^T, 1]^T \triangleq \bar{\phi} \in \mathbb{C}^{(N+1) \times 1}$. Similarly,

$$h_2 + \mathbf{v}\Phi\mathbf{g}_2 = h_2 + \mathbf{v}\text{diag}(\mathbf{g}_2)\phi = [\mathbf{v}\text{diag}(\mathbf{g}_2), h_2][\phi^T, 1]^T \triangleq \bar{\mathbf{g}}_2^H \bar{\phi}. \tag{26}$$

The problem $(\mathbf{Ps} - 2)$ is then equivalently transformed to

$$\begin{aligned}
 (\mathbf{Ps} - 3) : \max_{\phi} \quad & \min \{ |\bar{\mathbf{g}}_1^H \bar{\phi}|^2, |\bar{\mathbf{g}}_2^H \bar{\phi}|^2 \} \\
 \text{s.t.} \quad & |\phi_n| = 1, \forall n.
 \end{aligned} \tag{27}$$

By introducing an additional variable, denoted by t , the problem can be recast as follows:

$$\begin{aligned}
 (\mathbf{Ps} - 4) : \max_{\phi, t} \quad & t \\
 \text{s.t.} \quad & |\phi_n| = 1, \forall n,
 \end{aligned} \tag{28a}$$

$$\bar{\mathbf{g}}_1^H \bar{\phi} \bar{\phi}^H \bar{\mathbf{g}}_1 \geq t, \tag{28b}$$

$$\bar{\mathbf{g}}_2^H \bar{\phi} \bar{\phi}^H \bar{\mathbf{g}}_2 \geq t. \tag{28c}$$

Defining $\Psi \triangleq \bar{\phi} \bar{\phi}^H \in \mathbb{C}^{(N+1) \times (N+1)}$ where $\Psi \succeq 0$ and $\text{rank}(\Psi) = 1$, the semi-definite constraints in (28b) and (28c) become convex. Using Ψ and relaxing the rank-one constraint for Ψ , we can solve the following SDP problem:

$$\begin{aligned}
 (\mathbf{Ps} - 5) : \max_{\Psi, t} \quad & t \\
 \text{s.t.} \quad & \Psi[n, n] = 1, \forall n,
 \end{aligned} \tag{29a}$$

$$\Psi \succeq 0, \tag{29b}$$

$$\text{tr}[\Psi \bar{\mathbf{g}}_1 \bar{\mathbf{g}}_1^H] \geq t, \tag{29c}$$

$$\text{tr}[\Psi \bar{\mathbf{g}}_2 \bar{\mathbf{g}}_2^H] \geq t. \tag{29d}$$

Algorithm 1 Gaussian randomization procedure for obtaining the rank-one solution

- 1: Input: The solution of (Ps – 5): Ψ^*
 - 2: Perform singular value decomposition for Ψ^* as $\Psi^* = U_1^H \Sigma_1 U_1$.
 - 3: **if** Σ_1 is a rank-one matrix **then**
 - 4: $\bar{\phi}^* = U_1[1, :] \sqrt{\Sigma_1[1, 1]}$;
 - 5: **else**
 - 6: Initialize $\mathcal{D} = \emptyset$.
 - 7: **for** $d = 1 \rightarrow D$ **do**
 - 8: Generate random vectors $\phi_d = U_1^H \Sigma_1^{\frac{1}{2}} e_d$, where $e_d \sim \mathcal{CN}(0, \mathbf{I}_N)$.
 - 9: **if** ϕ_d satisfies the constraint of the Problem (Ps – 5) **then**
 - 10: $\mathcal{D} = \mathcal{D} \cup \phi_d$.
 - 11: Obtain the objective function value as Q_d .
 - 12: **end if**
 - 13: **end for**
 - 14: $\bar{\phi}^* = \arg \max_{d \in \mathcal{D}} Q_d$.
 - 15: **end if**
-

This SDP problem can be solved efficiently via CVX [40]. The optimal solution of Ψ , however, is not generally a rank-one matrix. Therefore, after obtaining the optimal Ψ from (Ps – 5), we need to find a rank-one solution by using the Gaussian randomization procedure as summarized in Algorithm 1. Once the optimal solution $\bar{\phi}^*$ is obtained, we obtain ϕ^* as

$$\phi^* = e^{j \arg \left(\left[\begin{array}{c} \bar{\phi}^* \\ \phi_{N+1}^* \end{array} \right]_{(1:N)} \right)}, \quad (30)$$

where $\arg(x)$ denotes the operation of taking the angle of the complex value x . The overall SUM algorithm is summarized in Algorithm 2.

B. Genetic-SNR-Maximization (GSM) Algorithm

RIS phase shift matrix Φ can be obtained from multiple candidates that maximize the minimum SNRs of the two users, which is a genetic algorithm. In the i th candidate generation, $\Phi^{(i-1)}$ represents the RIS phase shifts obtained in the previous generation and the denominators of

Algorithm 2 SUM algorithm to solve (Ps – 1)

- 1: Solve (Ps – 5) to obtain Ψ .
 - 2: Use Algorithm 1 to perform Gaussian randomization procedure for Ψ and obtain new $\bar{\phi}$.
 - 3: Obtain ϕ^* from (30).
 - 4: Obtain τ^* from (21).
 - 5: Return ϕ^* and τ^* .
-

SNRs in (23) are approximated by using the previously generated phase shift matrix as follows:

$$\eta_1^{(i)} \approx 1 + \frac{P_S}{P_B} + \frac{P_S |h_2 + \mathbf{v}\Phi^{(i-1)}\mathbf{g}_2|^2 + \sigma^2}{P_B |h_1 + \mathbf{v}\Phi^{(i-1)}\mathbf{g}_1|^2}, \quad (31)$$

$$\eta_2^{(i)} \approx 1 + \frac{P_S}{P_B} + \frac{P_S |h_1 + \mathbf{v}\Phi^{(i-1)}\mathbf{g}_1|^2 + \sigma^2}{P_B |h_2 + \mathbf{v}\Phi^{(i-1)}\mathbf{g}_2|^2}. \quad (32)$$

The i th genetic SNR maximization problem is then formulated as follows:

$$\begin{aligned} (\mathbf{Ps} - 6) : \max_{\Phi^{(i)}} \quad & \min \left\{ \frac{|h_1 + \mathbf{v}\Phi^{(i)}\mathbf{g}_1|^2}{\eta_2^{(i)}}, \frac{|h_2 + \mathbf{v}\Phi^{(i)}\mathbf{g}_2|^2}{\eta_1^{(i)}} \right\} \\ \text{s.t.} \quad & |\phi_n| = 1, \forall n. \end{aligned} \quad (33)$$

The above problem can be recast as

$$\begin{aligned} (\mathbf{Ps} - 7) : \max_{\Psi^{(i)}, t} \quad & t \\ \text{s.t.} \quad & \Psi^{(i)}[n, n] = 1, \forall n, \end{aligned} \quad (34a)$$

$$\Psi^{(i)} \succeq 0, \quad (34b)$$

$$\text{tr}[\Psi^{(i)}\bar{\mathbf{g}}_1\bar{\mathbf{g}}_1^H] \geq \eta_2^{(i)}t, \quad (34c)$$

$$\text{tr}[\Psi^{(i)}\bar{\mathbf{g}}_2\bar{\mathbf{g}}_2^H] \geq \eta_1^{(i)}t. \quad (34d)$$

This problem can be solved via CVX. In the GSM algorithm, we first initialize the RIS phase shifts ϕ and τ with the solution obtained in Algorithm 2. We then calculate $\eta_1^{(i)}$ and $\eta_2^{(i)}$ with the solution obtained in the previous generation and solve a problem (P7 – S) to obtain updated Ψ . A rank-one solution is found by following Algorithm 1 and ϕ^* is given by (30). We repeat the generation steps and record the minimum SNR until the fixed number of generations is reached. Finally, after the candidate generation, we choose the ϕ^* that maximizes the minimum SNR as the optimal solution. The overall GSM algorithm is summarized in Algorithm 3.

Algorithm 3 GSM algorithm to solve (Ps – 1)

- 1: Initialize Φ with the solution obtained in Algorithm 2. I is the candidate generation number.
 - 2: **for** $i = 1 \rightarrow I$ **do**
 - 3: Calculate $\eta_1^{(i)}$ and $\eta_2^{(i)}$ by (31) and (32).
 - 4: Solve (Ps – 7) to update $\Psi^{(i)}$.
 - 5: Use Algorithm 1 to perform Gaussian randomization procedure for $\Psi^{(i)}$ and obtain new $\bar{\phi}^{(i)}$.
 - 6: Obtain $\phi^{(i)}$ from (30).
 - 7: Obtain $\tau^{(i)}$ from (21).
 - 8: Record the minimum SNR and the corresponding $\phi^{(i)}$ and $\tau^{(i)}$.
 - 9: **end for**
 - 10: Choose ϕ^* and τ^* that maximize the minimum SNR.
 - 11: Return ϕ^* and τ^* .
-

C. Complexity Analysis

In the SUM algorithm, the problem (Ps – 5) is solved by using CVX and Gaussian randomization procedure. In the GSM algorithm, the problem (Ps – 7) is continuously solved until the maximal generation number is reached. Therefore, following the complexity analysis of a typical interior-point method like a primal-dual path-following method [41], the complexity of the SUM algorithm is $\mathcal{O}((N + 3)^4(N + 1)^{\frac{1}{2}}\log(\frac{1}{\epsilon_s}))$, whereas that of the GSM algorithm is $\mathcal{O}((1 + I)(N + 3)^4(N + 1)^{\frac{1}{2}}\log(\frac{1}{\epsilon_s}))$, where ϵ_s is the predefined solution accuracy and I is the candidate generation number in the GSM algorithm.

Remark 2: The SUM algorithm is a one-step algorithm, whereas the GSM algorithm is a genetic algorithm that repeatedly generates the candidates of the solution and initialized with the solution obtained in the SUM algorithm. Genetic algorithms are commonly used to generate high-quality solutions to optimization and search problems by relying on biologically inspired operations, such as mutation, crossover, and selection. In practical scenarios, the candidate generation number is not large. By setting different candidate generation numbers, we are able to balance the complexity and the performance. Specifically, to obtain better performance, we can

set the candidate generation number large to allow further exploration in the genetic algorithms. When the phase shift and beamforming matrices have to be updated frequently, we may set the candidate generation number small to reduce the complexity. The SUM algorithm is much simpler, whereas the GSM algorithm can achieve better performance at the cost of computational complexity. By proposing the SUM and GSM algorithms, we aim to achieve a favorable tradeoff between performance and complexity.

Remark 3: From the optimization for the single-antenna BS case case, we can obtain insight into how to maximize the upper bound of the SNR to obtain the optimal phase shift matrix. Furthermore, we can obtain the optimal power amplification parameter in a closed-form under the single-antenna BS case. On the other hand, for the multiple-antenna BS case, we need to optimize both beamforming and phase shift matrices.

IV. RIS FOR MULTIPLE-ANTENNA BS

In this section, we propose algorithms to design a phase shift matrix of RIS and a beamforming matrix of multiple-antenna BS. To solve the original problem (Po) in (17), it is divided into two subproblems, namely one for the RIS phase shift matrix and the other one for the BS beamforming matrix. Following the similar optimization procedure in Section III, an SUM-OB algorithm is devised. We then provide a low complexity method to obtain the beamforming matrix by utilizing a maximal-ratio-reception maximal-ratio-transmission (MRR-MRT) relaying scheme in [23] and propose the SUM-MRB algorithm. The GSM-OB and GSM-MRB algorithms are also developed to obtain the phase shifts Φ and the beamforming matrix \mathbf{A} by using a genetic algorithm for the case of multiple-antenna BS in TWRN.

A. SUM-OB Algorithm

1) *Phase Shift Optimization:* From (A1), the SNR upper bounds of S1 and S2 are $\beta \|\mathbf{h}_2 + \mathbf{V}\Phi\mathbf{g}_2\|^2$ and $\beta \|\mathbf{h}_1 + \mathbf{V}\Phi\mathbf{g}_1\|^2$, respectively. Similarly to the single-antenna BS case, an optimization problem to find the optimal phase shift matrix that can maximize the upper bound of minimum SNR of users for the multiple-antenna BS case can be formulated as follows:

$$\begin{aligned}
 (\mathbf{Pm} - \mathbf{a1}) : \max_{\Phi} \quad & \min \{ \|\mathbf{h}_1 + \mathbf{V}\Phi\mathbf{g}_1\|^2, \|\mathbf{h}_2 + \mathbf{V}\Phi\mathbf{g}_2\|^2 \} \\
 \text{s.t.} \quad & |\phi_n| = 1, \forall n.
 \end{aligned} \tag{35}$$

We note that the maximization of the upper bound of SNR conveys physical meaning. The more the combined channel gain is, the larger the SNR becomes. By introducing an additional variable Q and replacing the variable Φ with $\bar{\phi}$, the problem is further transformed to the following rank-relaxed SDP problem:

$$\begin{aligned} (\mathbf{Pm} - \mathbf{a2}) : \max_{\Psi, Q} \quad & Q \\ \text{s.t.} \quad & \Psi[n, n] = 1, \forall n, \end{aligned} \quad (36a)$$

$$\Psi \succeq 0, \quad (36b)$$

$$\text{tr}[\Psi \bar{\mathbf{G}}_1^H \bar{\mathbf{G}}_1] \geq Q, \quad (36c)$$

$$\text{tr}[\Psi \bar{\mathbf{G}}_2^H \bar{\mathbf{G}}_2] \geq Q. \quad (36d)$$

The SDP problem $(\mathbf{Pm} - \mathbf{a2})$ can be efficiently solved via CVX. From the optimal Ψ of (36), optimal rank-one solution ϕ^* is obtained from Algorithm 1 and (30).

2) *Beamforming Matrix Optimization:* After obtaining phase shift matrix Φ for RIS, the original problem (\mathbf{Po}) is transformed to

$$\begin{aligned} (\mathbf{Pm} - \mathbf{b1}) : \max_{\mathbf{A}} \quad & \min \{\gamma_1, \gamma_2\} \\ \text{s.t.} \quad & (14), (15), \text{ and } (17b). \end{aligned}$$

Defining $\tilde{\mathbf{h}}_1 \triangleq \mathbf{h}_1 + \mathbf{V}\Phi\mathbf{g}_1 \in \mathbb{C}^{M \times 1}$ and $\tilde{\mathbf{h}}_2 \triangleq \mathbf{h}_2 + \mathbf{V}\Phi\mathbf{g}_2 \in \mathbb{C}^{M \times 1}$, problem $(\mathbf{Pm} - \mathbf{b1})$ is further rewritten as follows:

$$\begin{aligned} (\mathbf{Pm} - \mathbf{b2}) : \max_{\mathbf{A}} \quad & \min \left\{ \frac{|\tilde{\mathbf{h}}_1^T \mathbf{A} \tilde{\mathbf{h}}_2|^2}{\|\tilde{\mathbf{h}}_1^T \mathbf{A}\|^2 + 1}, \frac{|\tilde{\mathbf{h}}_2^T \mathbf{A} \tilde{\mathbf{h}}_1|^2}{\|\tilde{\mathbf{h}}_2^T \mathbf{A}\|^2 + 1} \right\} \\ \text{s.t.} \quad & P_S \|\mathbf{A} \tilde{\mathbf{h}}_1\|^2 + P_S \|\mathbf{A} \tilde{\mathbf{h}}_2\|^2 + \sigma^2 \text{tr}[\mathbf{A} \mathbf{A}^H] \leq P_B. \end{aligned} \quad (37)$$

By introducing an additional variable Q' , problem **(Pm – b2)** is recast as

$$\begin{aligned} \text{(Pm – b3)} : \max_{\mathbf{A}, Q'} \quad & Q' \\ \text{s.t.} \quad & \frac{|\tilde{\mathbf{h}}_1^T \mathbf{A} \tilde{\mathbf{h}}_2|^2}{\|\tilde{\mathbf{h}}_1^T \mathbf{A}\|^2 + 1} \geq Q', \end{aligned} \quad (38a)$$

$$\frac{|\tilde{\mathbf{h}}_2^T \mathbf{A} \tilde{\mathbf{h}}_1|^2}{\|\tilde{\mathbf{h}}_2^T \mathbf{A}\|^2 + 1} \geq Q', \quad (38b)$$

(37).

By denoting $\text{vec}(\mathbf{A}) = \mathbf{a} \in \mathbb{C}^{M^2 \times 1}$, we have

$$\begin{aligned} |\tilde{\mathbf{h}}_1^T \mathbf{A} \tilde{\mathbf{h}}_2|^2 &= \text{tr} \left[(\tilde{\mathbf{h}}_1^T \mathbf{A} \tilde{\mathbf{h}}_2)^H \tilde{\mathbf{h}}_1^T \mathbf{A} \tilde{\mathbf{h}}_2 \right] = \text{vec} \left(\tilde{\mathbf{h}}_1^T \mathbf{A} \tilde{\mathbf{h}}_2 \right)^H \text{vec} \left(\tilde{\mathbf{h}}_1^T \mathbf{A} \tilde{\mathbf{h}}_2 \right) \\ &= \text{vec}(\mathbf{A})^H \left(\tilde{\mathbf{h}}_2^T \otimes \tilde{\mathbf{h}}_1^T \right)^H \left(\tilde{\mathbf{h}}_2^T \otimes \tilde{\mathbf{h}}_1^T \right) \text{vec}(\mathbf{A}) = \mathbf{a}^H \mathbf{C}_1 \mathbf{a}, \end{aligned} \quad (39)$$

$$\begin{aligned} \|\tilde{\mathbf{h}}_1^T \mathbf{A}\|^2 &= \text{vec}(\tilde{\mathbf{h}}_1^T \mathbf{A})^H \text{vec}(\tilde{\mathbf{h}}_1^T \mathbf{A}) = \text{vec}(\mathbf{A})^H \left(\mathbf{I} \otimes \tilde{\mathbf{h}}_1^T \right)^H \left(\mathbf{I} \otimes \tilde{\mathbf{h}}_1^T \right) \text{vec}(\mathbf{A}) \\ &= \mathbf{a}^H \mathbf{D}_1 \mathbf{a}. \end{aligned} \quad (40)$$

Therefore, the first constraint (38a) can be rewritten as

$$\mathbf{a}^H (\mathbf{C}_1 - Q' \mathbf{D}_1) \mathbf{a} \geq Q'. \quad (41)$$

After applying the similar techniques to the other two constraints, (37) and (38b), the problem **(Pm – b3)** in (38) is transformed as follows:

$$\text{(Pm – b4)} : \max_{\mathbf{a}, Q'} \quad Q' \quad (42a)$$

$$\text{s.t.} \quad \mathbf{a}^H (\mathbf{C}_1 - Q' \mathbf{D}_1) \mathbf{a} \geq Q', \quad (42a)$$

$$\mathbf{a}^H (\mathbf{C}_2 - Q' \mathbf{D}_2) \mathbf{a} \geq Q', \quad (42b)$$

$$\mathbf{a}^H \mathbf{F} \mathbf{a} \leq P_B, \quad (42c)$$

where

$$\mathbf{C}_1 = \left(\tilde{\mathbf{h}}_2^T \otimes \tilde{\mathbf{h}}_1^T \right)^H \left(\tilde{\mathbf{h}}_2^T \otimes \tilde{\mathbf{h}}_1^T \right), \mathbf{D}_1 = \left(\mathbf{I} \otimes \tilde{\mathbf{h}}_1^T \right)^H \left(\mathbf{I} \otimes \tilde{\mathbf{h}}_1^T \right), \quad (43)$$

$$\mathbf{C}_2 = \left(\tilde{\mathbf{h}}_1^T \otimes \tilde{\mathbf{h}}_2^T \right)^H \left(\tilde{\mathbf{h}}_1^T \otimes \tilde{\mathbf{h}}_2^T \right), \mathbf{D}_2 = \left(\mathbf{I} \otimes \tilde{\mathbf{h}}_2^T \right)^H \left(\mathbf{I} \otimes \tilde{\mathbf{h}}_2^T \right), \quad (44)$$

$$\mathbf{F} = P_S \left(\tilde{\mathbf{h}}_1^T \otimes \mathbf{I} \right)^H \left(\tilde{\mathbf{h}}_1^T \otimes \mathbf{I} \right) + P_S \left(\tilde{\mathbf{h}}_2^T \otimes \mathbf{I} \right)^H \left(\tilde{\mathbf{h}}_2^T \otimes \mathbf{I} \right) + \sigma^2 \mathbf{I}. \quad (45)$$

Defining $\Xi \triangleq \mathbf{a}\mathbf{a}^H \in \mathbb{C}^{M^2 \times M^2}$ and relaxing the rank-one constraint for Ξ , optimization problem **(Pm – b4)** can be recast as follows:

$$\begin{aligned} \text{(Pm – b5)} : \max_{\Xi, Q'} \quad & Q' \\ \text{s.t.} \quad & \Xi \succeq 0, \end{aligned} \tag{46a}$$

$$\text{tr} [\Xi (\mathbf{C}_1 - Q' \mathbf{D}_1)] \geq Q', \tag{46b}$$

$$\text{tr} [\Xi (\mathbf{C}_2 - Q' \mathbf{D}_2)] \geq Q', \tag{46c}$$

$$\text{tr} [\Xi \mathbf{F}] \leq P_B. \tag{46d}$$

This problem is still non-convex because Q' and Ξ are coupled, yet it is convex with respect to each of Q' and Ξ . Thus, we find the solution by using a convex feasibility problem test [42]. First, we obtain Q_{low} and Q_{up} of Q' where Q_{low} makes the problem **(Pm – b5)** feasible and Q_{up} makes the problem **(Pm – b5)** infeasible. We then calculate $Q_{new} = \frac{Q_{up} + Q_{low}}{2}$ and test the feasibility of the problem **(Pm – b5)** by replacing Q' with Q_{new} . If Q_{new} makes the problem feasible, we update $Q_{low} = Q_{new}$; otherwise, we update $Q_{up} = Q_{new}$. These steps are repeated until a stopping criterion is met. For a certain Q' , the problem is an SDP problem. Ξ can be obtained by solving the feasibility problem via CVX. With Ξ , Algorithm 1 performs the Gaussian randomization procedure to obtain \mathbf{a} , and the beamforming matrix \mathbf{A} can be recovered from \mathbf{a} by reshaping \mathbf{a} as an $M \times M$ matrix. The detailed steps of the SUM-OB algorithm are summarized in Algorithm 4.

B. SUM-MRB Algorithm

Since the computational complexity to obtain the beamforming matrix \mathbf{A} is high, a low-complexity SUM-MRB algorithm is devised. In the SUM-MRB algorithm, RIS phase shift matrix Φ is obtained through the same method as the SUM-OB algorithm, whereas beamforming matrix \mathbf{A} is obtained through an MRR-MRT relaying scheme in [23].

Defining $\mathbf{H}_1 \triangleq [\mathbf{h}_1 + \mathbf{V}\Phi\mathbf{g}_1, \mathbf{h}_2 + \mathbf{V}\Phi\mathbf{g}_2] \in \mathbb{C}^{M \times 2}$ and $\mathbf{H}_2 \triangleq [\mathbf{h}_2 + \mathbf{V}\Phi\mathbf{g}_2, \mathbf{h}_1 + \mathbf{V}\Phi\mathbf{g}_1]^T \in \mathbb{C}^{2 \times M}$, beamforming matrix \mathbf{A} can be designed as follows [23]:

$$\mathbf{A} = \alpha \mathbf{H}_2^H \mathbf{H}_1^H = \alpha \left(\bar{\mathbf{G}}_2 \bar{\phi} \bar{\phi}^T \bar{\mathbf{G}}_1^T + \bar{\mathbf{G}}_1 \bar{\phi} \bar{\phi}^T \bar{\mathbf{G}}_2^T \right)^* = \alpha \mathbf{A}_1, \tag{47}$$

Algorithm 4 SUM-OB algorithm to solve (Po)

- 1: Solve (Pm – a2) to obtain Ψ^* .
 - 2: Use Algorithm 1 to perform Gaussian randomization procedure for Ψ^* and obtain $\bar{\phi}^*$.
 - 3: Compute ϕ^* by (30).
 - 4: For given ϕ^* and Q_{low}, Q_{up} ,
 - 5: **while** $Q_{up} - Q_{low} \geq \epsilon_1$ **do**
 - 6: Calculate $Q_{new} = \frac{Q_{up} + Q_{low}}{2}$.
 - 7: Solve the feasibility problem (Pm – b5) with given $Q' = Q_{new}$.
 - 8: **if** the problem is feasible **then**
 - 9: $Q_{low} = Q_{new}$, update Ξ .
 - 10: **else**
 - 11: $Q_{up} = Q_{new}$.
 - 12: **end if**
 - 13: **end while**
 - 14: Obtain Ξ^* .
 - 15: Use Algorithm 1 to perform Gaussian randomization procedure for Ξ^* and obtain \mathbf{a} .
 - 16: Recover \mathbf{A}^* from \mathbf{a} .
 - 17: Return ϕ^* and \mathbf{A}^* .
-

where α is used to satisfy the power constraint with the equality in (17b). Specifically, α is derived as

$$\alpha = \sqrt{\frac{P_B}{P_S \text{tr} \left[\mathbf{A}_1 \left(\bar{\mathbf{G}}_1 \Psi \bar{\mathbf{G}}_1^H + \bar{\mathbf{G}}_2 \Psi \bar{\mathbf{G}}_2^H \right) \mathbf{A}_1^H \right] + \sigma^2 \text{tr} \left[\mathbf{A}_1 \mathbf{A}_1^H \right]}}. \quad (48)$$

In (47), \mathbf{H}_1^H corresponds to receive beamforming at BS, which maximizes the received energy along the direction of $\mathbf{h}_1 + \mathbf{V} \Phi \mathbf{g}_1$ and $\mathbf{h}_2 + \mathbf{V} \Phi \mathbf{g}_2$, and \mathbf{H}_2^H corresponds to transmit beamforming, which maximizes the transmission energy along the direction of $(\mathbf{h}_2 + \mathbf{V} \Phi \mathbf{g}_2)^T$ from BS to S2 and $(\mathbf{h}_1 + \mathbf{V} \Phi \mathbf{g}_1)^T$ from BS to S1. This scheme is called an MRR-MRT relaying scheme.

The SUM-MRB algorithm that employs the MRR-MRT to obtain the beamforming matrix is summarized in Algorithm 5. We note that both SUM-OB and the SUM-MRB algorithms are a one-step algorithm. In the next subsection, we will present the genetic algorithms, namely,

Algorithm 5 SUM-MRB algorithm to solve (Po)

- 1: Solve (Pm – a2) to obtain Ψ^* .
 - 2: Use Algorithm 1 to perform Gaussian randomization procedure for Ψ^* and obtain $\bar{\phi}^*$.
 - 3: Compute ϕ^* by (30).
 - 4: Compute A^* by (47) and (48).
 - 5: Return ϕ^* and A^* .
-

GSM-OB and GSM-MRB algorithms, for the multiple-antenna BS case.

C. GSM-OB and GSM-MRB Algorithms

In the GSM-OB algorithm, we obtain RIS phase shift matrix Φ and beamforming matrix A by consequently maximizing the SNRs of the two users. In the i th generation, denoting the RIS phase shift and beamforming matrices by $\Phi^{(i-1)}$ and $A^{(i-1)}$, respectively, in the previous generation, we obtain $\nu_1^{(i)} \in \mathbb{C}^{1 \times M}$, $\nu_2^{(i)} \in \mathbb{C}^{1 \times M}$, $\zeta_1^{(i)}$, and $\zeta_2^{(i)}$ as follows:

$$\nu_1^{(i)} = \left(\mathbf{h}_1 + \mathbf{V}\Phi^{(i-1)}\mathbf{g}_1 \right)^T A^{(i-1)}, \quad \nu_2^{(i)} = \left(\mathbf{h}_2 + \mathbf{V}\Phi^{(i-1)}\mathbf{g}_2 \right)^T A^{(i-1)}, \quad (49)$$

$$\zeta_1^{(i)} = \left\| \nu_1^{(i)} \right\|^2 + 1, \quad \zeta_2^{(i)} = \left\| \nu_2^{(i)} \right\|^2 + 1. \quad (50)$$

The SNRs for S1 and S2 are written as

$$\gamma_1^{(i)} = \frac{\beta \left| \nu_1^{(i)} \left(\mathbf{h}_2 + \mathbf{V}\Phi^{(i)}\mathbf{g}_2 \right) \right|^2}{\zeta_1^{(i)}} = \frac{\beta \left| \nu_1^{(i)} \bar{\mathbf{G}}_2 \bar{\phi}^{(i)} \right|^2}{\zeta_1^{(i)}}, \quad (51)$$

$$\gamma_2^{(i)} = \frac{\beta \left| \nu_2^{(i)} \left(\mathbf{h}_1 + \mathbf{V}\Phi^{(i)}\mathbf{g}_1 \right) \right|^2}{\zeta_2^{(i)}} = \frac{\beta \left| \nu_2^{(i)} \bar{\mathbf{G}}_1 \bar{\phi}^{(i)} \right|^2}{\zeta_2^{(i)}}. \quad (52)$$

The genetic SNR maximization problem of the i th generation is then formulated as follows:

$$\begin{aligned} (\mathbf{Pm} - \mathbf{a3}) : \max_{\Phi^{(i)}} \quad & \min \left\{ \frac{\left| \nu_1^{(i)} \bar{\mathbf{G}}_2 \bar{\phi}^{(i)} \right|^2}{\zeta_1^{(i)}}, \frac{\left| \nu_2^{(i)} \bar{\mathbf{G}}_1 \bar{\phi}^{(i)} \right|^2}{\zeta_2^{(i)}} \right\} \\ \text{s.t.} \quad & \left| \phi_n^{(i)} \right| = 1, \forall n. \end{aligned} \quad (53)$$

The problem can be transformed to the following rank-relaxed SDP problem:

$$(\mathbf{Pm} - \mathbf{a4}) : \max_{\Psi^{(i)}, Q} Q$$

$$\text{s.t. } \Psi^{(i)}[n, n] = 1, \forall n, \quad (54a)$$

$$\Psi^{(i)} \succeq 0, \quad (54b)$$

$$\text{tr} \left[\Psi^{(i)} \bar{\mathbf{G}}_1^H (\nu_2^{(i)})^H \nu_2^{(i)} \bar{\mathbf{G}}_1 \right] \geq \zeta_2^{(i)} Q, \quad (54c)$$

$$\text{tr} \left[\Psi^{(i)} \bar{\mathbf{G}}_2^H (\nu_1^{(i)})^H \nu_1^{(i)} \bar{\mathbf{G}}_2 \right] \geq \zeta_1^{(i)} Q. \quad (54d)$$

This problem ($\mathbf{Pm} - \mathbf{a4}$) can be solved by using CVX. In the GSM-OB algorithm, we first initialize RIS phase shift vector ϕ and beamforming matrix \mathbf{A} with the solution obtained in Algorithm 4. We then calculate $\nu_1^{(i)}$, $\nu_2^{(i)}$, $\zeta_1^{(i)}$, and $\zeta_2^{(i)}$ with the solution obtained in the previous generation, and solve problem ($\mathbf{Pm} - \mathbf{a4}$) to update Ψ . A rank-one solution is obtained from Algorithm 1 and (30). The update of \mathbf{A} is obtained by solving a problem ($\mathbf{Pm} - \mathbf{b5}$). We repeat these steps and record the minimum SNR and corresponding solution in each generation. Finally, after completing the predetermined number of generations, we choose the ϕ^* and \mathbf{A}^* that maximize the minimum SNR as the optimal solution of a GSM-OB algorithm. The detailed steps of the GSM-OB algorithm are summarized in Algorithm 6.

We now describe the GSM-MRB algorithm. In Algorithm 6, i.e., a GSM-OB algorithm, by replacing the seventh step with computing \mathbf{A} by (47) and (48) and by initializing the starting point in the first step with the solution obtained in the SUM-MRB algorithm, we can implement the GSM-MRB algorithm. Since other steps of the GSM-MRB algorithm are the same as the GSM-OB algorithm, the detailed steps of GSM-MRB algorithm are omitted here.

D. Complexity Analysis

In the SUM-OB algorithm, sub-problem ($\mathbf{Pm} - \mathbf{a2}$) is solved and then the sub-problem ($\mathbf{P5} - \mathbf{b}$) is solved alternately. To be specific, the iteration number is $\log_2\left(\frac{Q_{up}-Q_{low}}{\epsilon_1}\right)$ to achieve an accuracy of ϵ_1 for Q . Hence, We can obtain the complexity order of the SUM-OB algorithm as $\mathcal{O}\left((N+3)^4(N+1)^{\frac{1}{2}}\log\left(\frac{1}{\epsilon_s}\right) + \log_2\left(\frac{Q_{up}-Q_{low}}{\epsilon_1}\right)M^9\log\left(\frac{1}{\epsilon_s}\right)\right)$. The SUM-MRB algorithm obtains the beamforming matrix with less complexity and the complexity is given by $\mathcal{O}\left((N+3)^4(N+1)^{\frac{1}{2}}\log\left(\frac{1}{\epsilon_s}\right) + 2M^3 + 4M^2(N+1) + 2M(N+1)^2\right)$. The GSM-OB and GSM-MRB algorithms are

Algorithm 6 GSM-OB algorithm to solve (Po)

- 1: Initialize Φ and \mathbf{A} with the solution obtained in Algorithm 4. I is the candidate generation number.
 - 2: **for** $i = 1 \rightarrow I$ **do**
 - 3: Calculate $\nu_1^{(i)}$, $\nu_2^{(i)}$, $\zeta_1^{(i)}$, and $\zeta_2^{(i)}$ by (49), (50).
 - 4: Solve (Pm – a4) to update $\Psi^{(i)}$.
 - 5: Use Algorithm 1 to perform Gaussian randomization procedure for $\Psi^{(i)}$ and update $\bar{\phi}^{(i)}$.
 - 6: Obtain $\phi^{(i)}$ from (30).
 - 7: Solve (Pm – b5) to update $\Xi^{(i)}$.
 - 8: Use Algorithm 1 to perform Gaussian randomization procedure for $\Xi^{(i)}$ and update $\mathbf{a}^{(i)}$.
 - 9: Recover $\mathbf{A}^{(i)}$ from $\mathbf{a}^{(i)}$.
 - 10: Record the minimum SNR and the corresponding $\phi^{(i)}$ and $\mathbf{A}^{(i)}$.
 - 11: **end for**
 - 12: Choose ϕ^* and \mathbf{A}^* that maximize the minimum SNR.
 - 13: Return ϕ^* and \mathbf{A}^* .
-

genetic algorithms and their computational complexity orders are analyzed as $\mathcal{O}\left((1+I)((N+3)^4(N+1)^{\frac{1}{2}}\log(\frac{1}{\epsilon_s}) + \log_2(\frac{Q_{up}-Q_{low}}{\epsilon_1})M^9\log(\frac{1}{\epsilon_s}))\right)$ and $\mathcal{O}\left((1+I)((N+3)^4(N+1)^{\frac{1}{2}}\log(\frac{1}{\epsilon_s}) + 2M^3 + 4M^2(N+1) + 2M(N+1)^2)\right)$, respectively.

Remark 4: For the multiple-antenna BS case, we propose four algorithms, namely the SUM-OB, SUM-MRB, GSM-OB, and GSM-MRB algorithms. Their relationships can be summarized in Table II. The SUM-OB and SUM-MRB algorithms are the one-step algorithms, whereas the GSM-OB and GSM-MRB algorithms are the genetic algorithms. From the complexity analysis, we can conclude that the SUM-MRB algorithm requires the least computational complexity, whereas the GSM-OB algorithm can achieve the best performance, as numerically verified in the next section. There exists a performance-and-complexity tradeoff between the proposed algorithms.

V. SIMULATION RESULTS

In this section, simulation results are provided to validate the effectiveness of the proposed algorithms. In the simulations, we consider a TWRN, in which the BS is equipped with four antennas and the RIS is a uniform rectangular array with 10×10 reflective elements. We set $d_{1,R} = 40$ m, $d_{2,R} = 60$ m, $d_{B,R} = 80$ m, $d_{B,1} = \sqrt{d_{1,R}^2 + d_{B,R}^2}$ and $d_{B,2} = \sqrt{d_{2,R}^2 + d_{B,R}^2}$. The system parameters are nearly identical to those in [43]. Specifically, the path loss is set according to the 3GPP Urban Micro (UMi) scenario from [44] with a carrier frequency of 2.5 GHz. The path loss is set as follows:

$$\beta(d)[\text{dB}] = \begin{cases} G_t + G_r - 35.95 - 22\log_{10}(d), & \text{for an LoS channel,} \\ G_t + G_r - 33.05 - 36.7\log_{10}(d), & \text{for an NLoS channel,} \end{cases} \quad (55)$$

where G_t and G_r denote the corresponding antenna gains (in dBi) at the transmitter and receiver, respectively. We assume that the BS and RIS have a gain of 5 dBi and the users have a gain of 0 dBi. The bandwidth $B = 180$ kHz, and the noise power $\sigma^2 = -174 + 10\log_{10}(B)$ dBm. We set the Rician factor $K_v = K_1 = K_2 = 10$. The center azimuth AoA is chosen randomly from $[-\pi, \pi]$, whereas the elevation AoA is chosen randomly from $[-25^\circ, 25^\circ]$. Simulation results are based on 10^3 random channel realizations.

A. RIS for Single-Antenna BS

The minimum SNRs of the proposed algorithms are evaluated when $P_S = 0$ dBm by varying the transmit power budget of BS with a single antenna. For comparison purpose, the following two benchmark schemes are considered.

- Benchmark 1 (RIS: random phase): The phase shifts are randomly chosen from $[0, 2\pi]$ and the power amplification parameter τ with which the BS amplifies its received signal is given by (21).
- Benchmark 2 (No RIS): A TWR system without RIS is considered and the power amplification parameter τ is given by $\tau = \frac{P_B}{P_S|h_1|^2 + P_S|h_2|^2 + \sigma^2}$.

Fig. 2 shows users' minimum SNR versus the transmit power budget for different algorithms. It is observed that the minimum SNR increases and is saturated as the transmit power budget increases. The minimum SNR saturation is owing to the extant additive noise. Besides, we observe that the performance gain by deploying the RIS is negligible if the phase shifts are

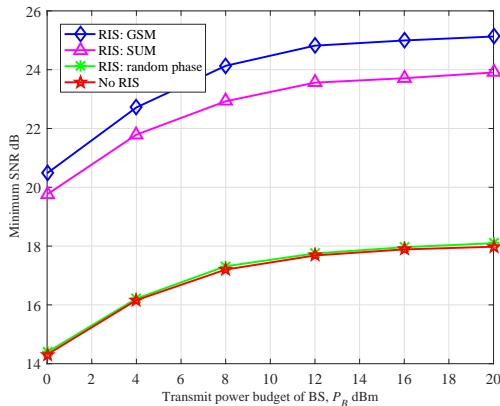


Fig. 2. Minimum SNR over transmit power budget of single-antenna BS when $P_S = 0$ dBm.

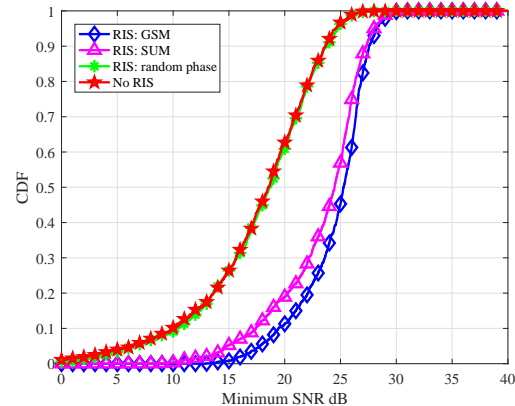


Fig. 3. CDF of minimum SNR for different algorithms when $P_B = 10$ dBm and $P_S = 0$ dBm.

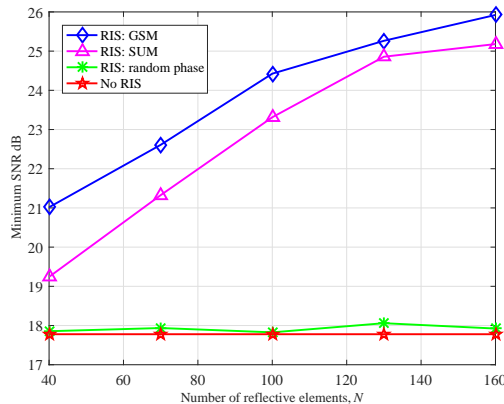


Fig. 4. Minimum SNR over the number of the reflective elements for the single-antenna BS case when $P_B = 10$ dBm and $P_S = 0$ dBm.

randomly chosen. Also, the proposed SUM and GSM algorithms can achieve approximately 5 dB and 6 dB gain, respectively, compared to the benchmark schemes. As expected, the GSM algorithm outperforms the SUM algorithm at the cost of the computational complexity.

Fig. 3 shows the *cumulative distribution function* (CDF) of the minimum SNR for different algorithms when $P_B = 10$ dBm and $P_S = 0$ dBm. We can take the CDF as the user success probability and the minimum SNR as the users' target SNR. Here, the users' target SNR means both users can decode their information correctly if their real SNR is higher than this target SNR. The user success probability is referred to as the probability that the users can meet the SNR

constraints. When the minimum SNR takes the value of 20 dB, for example, the corresponding CDF value is 0.114, 0.188, 0.614, and 0.625 for the GSM, SUM, random phase RIS, and No RIS algorithms, respectively, which means that 11.4%, 18.8%, 61.4%, and 62.5% minimum SNRs obtained from the algorithms are lower than the target SNR, 20 dB. This validates the performance advantage of the proposed SUM and GSM algorithms. Moreover, the performance gains obtained from the proposed SUM and GSM algorithms are stable according to the CDF curve and consistent with the results in Fig. 3, which shows the superiority of the proposed algorithms.

Fig. 4 plots users' minimum SNR across the number of reflective elements, i.e., N , where $P_B = 10$ dBm and $P_S = 0$ dBm. Here, we set $N_h = 10$ and $N_v = 4, 7, 10, 13, 16$. As expected, we observe that the minimum SNR increases as N increases for the SUM and GSM algorithms. The performance gap between the proposed algorithms and benchmark schemes becomes larger as N increases.

B. RIS for Multiple-Antenna BS

The proposed algorithms for multi-antenna BS, namely SUM-OB, SUM-MRB, GSM-OB, and GSM-MRB, are compared to the following benchmark schemes:

- Benchmark scheme 1 (No RIS): Without the RIS deployed and we only optimize the beamforming matrix at BS. The beamforming matrix is obtained by (47) and (48).
- Benchmark scheme 2 (RIS: random phase-MRB): The phase shifts are randomly chosen, whereas the beamforming matrix is obtained by (47) and (48).

Fig. 5 shows users' minimum SNR across the transmit power budget for various algorithms. It is observed that the minimum SNR increases up to a certain level as P_B increases. As expected, the performances of the proposed algorithms outperform the benchmark schemes. Specifically, the SUM-MRB, SUM-OB, GSM-MRB, and GSM-OB algorithms can achieve the gain of approximately 2.9 dB, 3.5 dB, 3.7 dB, and 4.3 dB compared to the benchmark scheme without RIS. The GSM algorithms provide better performance compared to the SUM algorithms. The computational complexity reduction from MRB causes minimum SNR degradation marginally by approximately 0.7 dB, compared to the OB algorithm.

Fig. 6 illustrates the CDF of the minimum SNR for different algorithms, similarly to the single-antenna BS case when $P_B = 10$ dBm and $P_S = 0$ dBm. It is observed that, for the

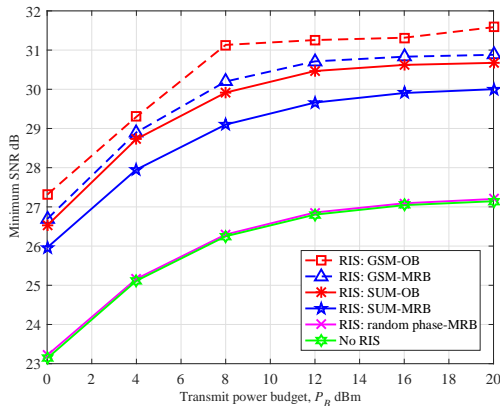


Fig. 5. Minimum SNR over transmit power budget for various algorithms for the multiple-antenna BS case when $P_S = 0$ dBm. Fig. 6. CDF of minimum SNR for different algorithms for the multiple-antenna BS case when $P_B = 10$ dBm and $P_S = 0$ dBm.

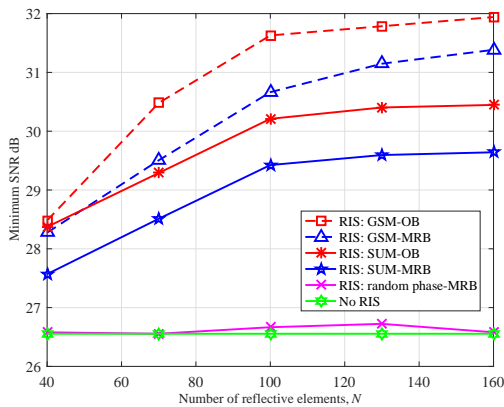
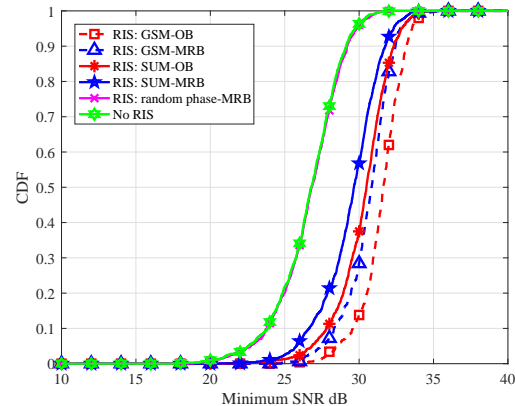
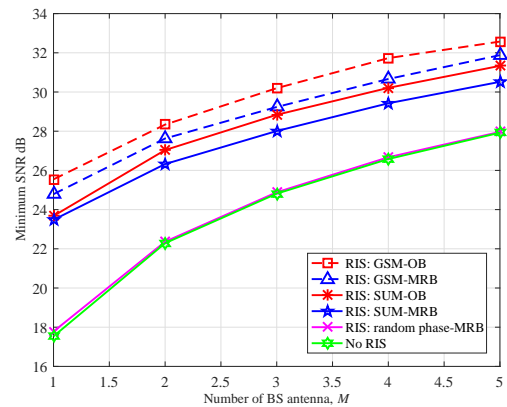


Fig. 7. Minimum SNR over the number of the reflective elements when $P_B = 10$ dBm and $P_S = 0$ dBm. Fig. 8. Minimum SNR over the number of the BS antennas, where $P_B = 10$ dBm and $P_S = 0$ dBm.



same user success probability, two users can decode information with a much stringent SNR constraint with the proposed algorithms, compared to the benchmark schemes. The performance gains of the proposed algorithms are also stable according to the CDF curve, which means that the proposed algorithms can perform well with high probability.

Fig. 7 shows users' minimum SNR over the number of reflective elements N for the multiple-antenna BS case when $P_B = 10$ dBm and $P_S = 0$ dBm. The minimum SNRs for the proposed algorithms increase as N increases, whereas the minimum SNRs of the benchmark schemes

remain unchanged.

Fig. 8 shows users' minimum SNR over the number of BS antennas, M , when $P_B = 10$ dBm and $P_S = 0$ dBm. As expected, the minimum SNR increases as M increases for all schemes since the beamforming gain of BS increases. Here, it should be emphasized that the proposed algorithms outperform the benchmark schemes irrespective of M .

VI. CONCLUSIONS

In this paper, an RIS-assisted TWRN was investigated and a joint beamforming and RIS design problem was formulated to maximize the minimum SNR under the transmit power constraint at the BS. The single-antenna BS case was first considered and addressed by devising the SUM and GSM algorithms. The optimization problem was then divided into two subproblems to design the phase shift and beamforming matrices for the case with a multiple-antenna BS. The RIS phase shift matrix was obtained by employing SUM or GSM method while the BS beamforming matrix was obtained by using OB or MRB method. Simulation results demonstrate that the proposed algorithms can achieve significant performance gains compared to the benchmark schemes, which validates the benefits of the RIS in TWRN.

APPENDIX A

PROOF OF PROPOSITION 1

Proof: From the Holder's inequality, (14) is bounded as follows:

$$\gamma_1 \leq \frac{\beta \left\| (\mathbf{h}_1 + \mathbf{V}\Phi_2\mathbf{g}_1)^T \mathbf{A} \right\|^2 \left\| \mathbf{h}_2 + \mathbf{V}\Phi_1\mathbf{g}_2 \right\|^2}{\left\| (\mathbf{h}_1 + \mathbf{V}\Phi_2\mathbf{g}_1)^T \mathbf{A} \right\|^2 + 1} = \frac{\beta \left\| \mathbf{h}_2 + \mathbf{V}\Phi_1\mathbf{g}_2 \right\|^2}{1 + \frac{1}{\left\| (\mathbf{h}_1 + \mathbf{V}\Phi_2\mathbf{g}_1)^T \mathbf{A} \right\|^2}} \quad (\text{A1})$$

Here, the equality holds when $\mathbf{A}^H \hat{\mathbf{h}}_1^*$ is parallel to $\hat{\mathbf{h}}_2$, i.e.,

$$\mathbf{A}^H \hat{\mathbf{h}}_1^* = \mu \hat{\mathbf{h}}_2, \quad (\text{A2})$$

where μ is a scalar, $\hat{\mathbf{h}}_1 \triangleq \mathbf{h}_1 + \mathbf{V}\Phi_2\mathbf{g}_1$, and $\hat{\mathbf{h}}_2 \triangleq \mathbf{h}_2 + \mathbf{V}\Phi_1\mathbf{g}_2$. Substituting the beamforming matrix structure \mathbf{A} in [23] into the equation, we obtain

$$(\hat{\mathbf{h}}_2 \hat{\mathbf{h}}_1^T + \hat{\mathbf{h}}_1 \hat{\mathbf{h}}_2^T) \hat{\mathbf{h}}_1^* = \mu \hat{\mathbf{h}}_2. \quad (\text{A3})$$

The first term of the left-hand side in (A3) is scaled $\hat{\mathbf{h}}_2$ and the second term is scaled $\hat{\mathbf{h}}_1$. The equality holds when $\hat{\mathbf{h}}_1 \perp \hat{\mathbf{h}}_2$ or $\hat{\mathbf{h}}_1 \parallel \hat{\mathbf{h}}_2$. $\hat{\mathbf{h}}_1$ and $\hat{\mathbf{h}}_2$ can be orthogonal when the number of the reflective elements is large. Similarly, we have

$$\gamma_2 \leq \frac{\beta \|\mathbf{h}_1 + \mathbf{V}\Phi_1\mathbf{g}_1\|^2}{1 + \frac{1}{\|(\mathbf{h}_2 + \mathbf{V}\Phi_2\mathbf{g}_2)^T \mathbf{A}\|^2}}. \quad (\text{A4})$$

It is observed that Φ_1 and Φ_2 are decoupled in the SNR term and that their optimization can be split into two subproblems. For Φ_1 , the larger $\|\mathbf{h}_2 + \mathbf{V}\Phi_1\mathbf{g}_2\|^2$ makes γ_1 larger. Therefore, the optimal Φ_1 is the solution of the problem which maximizes the minimum of $\|\mathbf{h}_1 + \mathbf{V}\Phi_1\mathbf{g}_1\|^2$ and $\|\mathbf{h}_2 + \mathbf{V}\Phi_1\mathbf{g}_2\|^2$. We have

$$\begin{aligned} \|(\mathbf{h}_1 + \mathbf{V}\Phi_2\mathbf{g}_1)^T \mathbf{A}\|^2 &= \|\hat{\mathbf{h}}_1^T \mathbf{A}\|^2 = \|\alpha \hat{\mathbf{h}}_1^T (\hat{\mathbf{h}}_2^* \hat{\mathbf{h}}_1^H + \hat{\mathbf{h}}_1^* \hat{\mathbf{h}}_2^H)\|^2 \\ &= \alpha^2 \|\hat{\mathbf{h}}_1^T \hat{\mathbf{h}}_2^* \hat{\mathbf{h}}_1^H + \hat{\mathbf{h}}_1^T \hat{\mathbf{h}}_1^* \hat{\mathbf{h}}_2^H\|^2 \geq \alpha^2 |\hat{\mathbf{h}}_1^T \hat{\mathbf{h}}_1^*|^2 \|\hat{\mathbf{h}}_2\|^2 \\ &= \alpha^2 |\hat{\mathbf{h}}_1^T \hat{\mathbf{h}}_1^*|^2 \|\mathbf{h}_2 + \mathbf{V}\Phi_2\mathbf{g}_2\|^2. \end{aligned} \quad (\text{A5})$$

Therefore, for Φ_2 , the larger $\|\mathbf{h}_2 + \mathbf{V}\Phi_2\mathbf{g}_2\|^2$ makes γ_1 larger. The optimal Φ_2 is also the solution of the problem which maximizes the minimum of $\|\mathbf{h}_1 + \mathbf{V}\Phi_2\mathbf{g}_1\|^2$ and $\|\mathbf{h}_2 + \mathbf{V}\Phi_2\mathbf{g}_2\|^2$. Therefore, the optimal RIS phase shift matrices in the first and second phases are identical to each other, i.e., $\Phi_1 = \Phi_2$. ■

REFERENCES

- [1] J. Wang, Y.-C. Liang, X. Yuan, and X. Wang, "Joint beamforming and reconfigurable intelligent surface design for two-way relay networks," in *Proc. IEEE Globecom*, Taipei, Taiwan, China, Dec. 2020, pp. 1–6.
- [2] X. You *et al.*, "Towards 6G wireless communication networks: Vision, enabling technologies, and new paradigm shifts," *Sci. China Inf. Sci.*, vol. 64, no. 1, pp. 1–74, 2021.
- [3] Y.-C. Liang, Q. Zhang, E. G. Larsson, and G. Y. Li, "Symbiotic radio: Cognitive backscattering communications for future wireless networks," *IEEE Trans. Cogn. Commun. Netw.*, vol. 6, no. 4, pp. 1242–1255, 2020.
- [4] L. Zhang, Y.-C. Liang, and D. Niyato, "6G visions: Mobile ultra-broadband, super internet-of-things, and artificial intelligence," *China Commun.*, vol. 16, no. 8, pp. 1–14, Aug. 2019.
- [5] Y.-C. Liang, *Dynamic Spectrum Management*. Springer Nature, 2020.
- [6] Y.-C. Liang, R. Long, Q. Zhang, J. Chen, H. V. Cheng, and H. Guo, "Large intelligent surface/antennas (LISA): Making reflective radios smart," *J. Commn. Inf. Netw.*, vol. 4, no. 2, pp. 40–50, June 2019.
- [7] S. Gong, X. Lu, D. T. Hoang, D. Niyato, L. Shu, D. I. Kim, and Y.-C. Liang, "Toward smart wireless communications via intelligent reflecting surfaces: A contemporary survey," *IEEE Commun. Surv. Tutor.*, vol. 22, no. 4, pp. 2283–2314, 2020.
- [8] E. Basar, M. Di Renzo, J. De Rosny, M. Debbah, M. Alouini, and R. Zhang, "Wireless communications through reconfigurable intelligent surfaces," *IEEE Access*, vol. 7, pp. 116 753–116 773, 2019.

- [9] C. Huang, A. Zappone, G. C. Alexandropoulos, M. Debbah, and C. Yuen, "Reconfigurable intelligent surfaces for energy efficiency in wireless communication," *IEEE Trans. Wireless Commun.*, vol. 18, no. 8, pp. 4157–4170, June 2019.
- [10] J. Chen, Y.-C. Liang, Y. Pei, and H. Guo, "Intelligent reflecting surface: A programmable wireless environment for physical layer security," *IEEE Access*, vol. 7, pp. 82 599–82 612, 2019.
- [11] X. Guan, Q. Wu, and R. Zhang, "Intelligent reflecting surface assisted secrecy communication: Is artificial noise helpful or not?" *IEEE Wireless Commun. Lett.*, vol. 9, no. 6, pp. 778–782, 2020.
- [12] H. Guo, Y.-C. Liang, J. Chen, and E. G. Larsson, "Weighted sum-rate maximization for reconfigurable intelligent surface aided wireless networks," *IEEE Trans. Wireless Commun.*, Feb. 2020.
- [13] H. Xie, J. Xu, and Y.-F. Liu, "Max-min fairness in IRS-aided multi-cell MISO systems with joint transmit and reflective beamforming," *IEEE Trans. Wireless Commun.*, vol. 20, no. 2, pp. 1379–1393, 2021.
- [14] D. Xu, X. Yu, Y. Sun, D. W. K. Ng, and R. Schober, "Resource allocation for IRS-assisted full-duplex cognitive radio systems," *IEEE Trans. Commun.*, vol. 68, no. 12, pp. 7376–7394, 2020.
- [15] H. Han, J. Zhao, D. Niyato, M. Di Renzo, and Q.-V. Pham, "Intelligent reflecting surface aided network: Power control for physical-layer broadcasting," *arXiv preprint arXiv:1910.14383*, 2019.
- [16] G. Zhou, C. Pan, H. Ren, K. Wang, and A. Nallanathan, "Intelligent reflecting surface aided multigroup multicast MISO communication systems," *IEEE Trans. Signal Process.*, vol. 68, pp. 3236–3251, 2020.
- [17] Q. Zhang, Y.-C. Liang, and H. V. Poor, "Large intelligent surface/antennas (LISA) assisted symbiotic radio for IoT communications," *arXiv preprint arXiv:2002.00340*, 2020.
- [18] G. Yang, X. Xu, and Y.-C. Liang, "Intelligent reflecting surface assisted non-orthogonal multiple access," *arXiv preprint arXiv:1907.03133*, 2019.
- [19] Z. Ding and H. V. Poor, "A simple design of IRS-NOMA transmission," *IEEE Commun. Lett.*, vol. 24, no. 5, pp. 1119–1123, 2020.
- [20] P. Wang, J. Fang, X. Yuan, Z. Chen, and H. Li, "Intelligent reflecting surface-assisted millimeter wave communications: Joint active and passive precoding design," *IEEE Trans. Veh. Technol.*, vol. 69, no. 12, pp. 14 960–14 973, 2020.
- [21] N. S. Perović, M. Di Renzo, and M. F. Flanagan, "Channel capacity optimization using reconfigurable intelligent surfaces in indoor mmwave environments," *arXiv preprint arXiv:1910.14310*, 2019.
- [22] B. Rankov and A. Wittneben, "Spectral efficient protocols for half-duplex fading relay channels," *IEEE J. Sel. Areas Commun.*, vol. 25, no. 2, pp. 379–389, Feb. 2007.
- [23] Y.-C. Liang and R. Zhang, "Optimal analogue relaying with multi-antennas for physical layer network coding," in *Proc. IEEE ICC*, Beijing, China, May 2008, pp. 3893–3897.
- [24] R. Zhang, Y.-C. Liang, C. C. Chai, and S. Cui, "Optimal beamforming for two-way multi-antenna relay channel with analogue network coding," *IEEE J. Sel. Areas Commun.*, vol. 27, no. 5, pp. 699–712, June 2009.
- [25] W. Wang, S. Jin, and F.-C. Zheng, "Maximin SNR beamforming strategies for two-way relay channels," *IEEE Commun. Lett.*, vol. 16, no. 7, pp. 1006–1009, May 2012.
- [26] Z. Fang, X. Wang, and X. Yuan, "Beamforming design for multiuser two-way relaying: A unified approach via max-min SINR," *IEEE Trans. Signal Process.*, vol. 61, no. 23, pp. 5841–5852, Sept. 2013.
- [27] J. Joung and A. H. Sayed, "Multiuser two-way amplify-and-forward relay processing and power control methods for beamforming systems," *IEEE Trans. Signal Process.*, vol. 58, no. 3, pp. 1833–1846, Dec. 2009.
- [28] Y. Zhang, C. Zhong, Z. Zhang, and W. Lu, "Sum rate optimization for two way communications with intelligent reflecting surface," *IEEE Commun. Lett.*, vol. 24, no. 5, pp. 1090–1094, Mar. 2020.

- [29] S. Atapattu, R. Fan, P. Dharmawansa, G. Wang, J. Evans, and T. A. Tsiftsis, "Reconfigurable intelligent surface assisted two-way communications: Performance analysis and optimization," *IEEE Trans. Commun.*, vol. 68, no. 10, pp. 6552–6567, 2020.
- [30] Z. Peng, Z. Zhang, C. Pan, L. Li, and A. L. Swindlehurst, "Multiuser full-duplex two-way communications via intelligent reflecting surface," *IEEE Trans. Signal Process.*, vol. 69, pp. 837–851, 2021.
- [31] C. Pradhan, A. Li, L. Song, B. Vucetic, and Y. Li, "Hybrid precoding design for reconfigurable intelligent surface aided mmwave communication systems," *IEEE Wireless Commun. Lett.*, vol. 9, no. 7, pp. 1041–1045, 2020.
- [32] H. Liu, X. Yuan, and Y. J. Zhang, "Super-resolution blind channel-and-signal estimation for massive MIMO with one-dimensional antenna array," *IEEE Trans. Signal Process.*, vol. 67, no. 17, pp. 4433–4448, July 2019.
- [33] G. Levin and S. Loyka, "Amplify-and-forward versus decode-and-forward relaying: Which is better?" in *22th International Zurich seminar on communications (IZS)*. Eidgenössische Technische Hochschule Zürich, 2012.
- [34] F. Gao, R. Zhang, and Y.-C. Liang, "Optimal channel estimation and training design for two-way relay networks," *IEEE Trans. Commun.*, vol. 57, no. 10, pp. 3024–3033, 2009.
- [35] S. Wang, M. Xia, and Y.-C. Wu, "Multipair two-way relay network with harvest-then-transmit users: resolving pairwise uplink-downlink coupling," *IEEE J. Sel. Topics Signal Process.*, vol. 10, no. 8, pp. 1506–1521, 2016.
- [36] Q.-U.-A. Nadeem, A. Kammoun, A. Chaaban, M. Debbah, and M.-S. Alouini, "Intelligent reflecting surface assisted multi-user MISO communication," *arXiv preprint arXiv:1906.02360*, 2019.
- [37] Z. He and X. Yuan, "Cascaded channel estimation for large intelligent metasurface assisted massive MIMO," *IEEE Wireless Commun. Lett.*, vol. 9, no. 2, pp. 210–214, Oct. 2020.
- [38] A. Taha, M. Alrabeiah, and A. Alkhateeb, "Enabling large intelligent surfaces with compressive sensing and deep learning," *arXiv preprint arXiv:1904.10136*, 2019.
- [39] J. Wang, Y.-C. Liang, S. Han, and Y. Pei, "Robust beamforming and phase shift design for IRS-enhanced multi-user MISO downlink communication," in *Proc. IEEE ICC*, Dublin, Ireland, June 2020, pp. 1–6.
- [40] M. Grant and S. Boyd, "CVX: MATLAB software for disciplined convex programming, version 2.1," 2014.
- [41] C. Helmberg, F. Rendl, R. J. Vanderbei, and H. Wolkowicz, "An interior-point method for semidefinite programming," *SIAM J. Optim.*, vol. 6, no. 2, pp. 342–361, 1996.
- [42] J. Joung, Y. K. Chia, and S. Sun, "Energy-efficient, large-scale distributed-antenna system (L-DAS) for multiple users," *J. Sel. Topics Signal Process.*, vol. 8, no. 5, pp. 954–965, Mar. 2014.
- [43] A. Kammoun, A. Chaaban, M. Debbah, M.-S. Alouini, *et al.*, "Asymptotic max-min SINR analysis of reconfigurable intelligent surface assisted MISO systems," *IEEE Trans. Wireless Commun.*, vol. 19, no. 12, pp. 7748–7764, 2020.
- [44] "Further advancements for E-UTRA physical layer aspects," *3GPP Technical Specification TR*, vol. 36, p. V2, 2010.